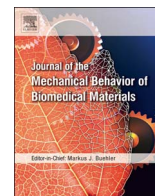




Contents lists available at ScienceDirect

Journal of the Mechanical Behavior of Biomedical Materials

journal homepage: www.elsevier.com/locate/jmbbm

Effects of non-enzymatic glycation on the micro- and nano-mechanics of articular cartilage



Parisa R. Moshtagh^{a,b,*}, Nicoline M. Korthagen^{a,d}, Mattie H.P. van Rijen^a, Rene M. Castelein^a, Amir A. Zadpoor^b, Harrie Weinans^{a,b,c}

^a Department of Orthopaedics, University Medical Center Utrecht, Utrecht, The Netherlands

^b Faculty of Mechanical, Maritime, and Materials Engineering, Delft University of Technology (TU Delft), Mekelweg 2, Delft 2628 CD, The Netherlands

^c Department of Rheumatology, University Medical Center Utrecht, Utrecht, The Netherlands

^d Department of Equine Sciences, Faculty of Veterinary Medicine, Utrecht University, Utrecht, The Netherlands

ARTICLE INFO

Keywords:

Articular cartilage
Advanced glycation
Nano-stiffness
Micro-stiffness

ABSTRACT

The mechanical properties of articular cartilage depend on the quality of its matrix, which consists of collagens and glycosaminoglycans (GAGs). The accumulation of advanced glycation end products (AGEs) can greatly affect the mechanics of cartilage. In the current study, we simulated the accumulation of AGEs by using L-threose to cross-link collagen molecules in the cartilage matrix (in vitro). The resulting changes in the mechanical properties (stiffness) of cartilage are then measured both at the micrometer-scale (using micro-indenter) and nanometer-scale (using indentation-type atomic force microscopy). Non-enzymatic cross-linking within the cartilage matrix was confirmed by the browning of L-threose-treated samples. We observed > 3 times increase in the micro-scale stiffness and up to 12-fold increase in the nano-scale stiffness of the glycated cartilage in the peak pertaining to the collagen fibers, which is caused by cartilage network embrittlement. At the molecular level, we found that besides the collagen component, the glycation process also influenced the GAG macromolecules. Comparing cartilage samples before and after L-threose treatment revealed that artificially induced-AGEs also decelerate in vitro degradation (likely via matrix metalloproteinases), observed at both micro- and nano-scales. The combined observations suggest that non-enzymatic glycation may play multiple roles in mechanochemical functioning of articular cartilage.

1. Introduction

Osteoarthritis (OA) is categorized as a chronic and complicated degenerative disorder of the joints in which the natural turnover of glycosaminoglycans (GAGs) in articular cartilage is disrupted (Ghosh and Smith, 2002). Irreversible structural damage is mainly detectable in the progressed stages of OA at tissue level, while early degradations are initiated at a small molecular-scale from the early stage OA (Stolz et al., 2009; Chu et al., 2012). Among different layers of cartilage multi-zonal structure, the superficial layer is the first affected zone under degenerative conditions (Sophia Fox et al., 2009). This underscores the importance of detecting the molecular-scale changes of the cartilage surface layer. Aging is considered one of the major risk factors of OA as age-related accumulation of advanced glycation end products (AGEs) affects the synthesis and degradation of the collagen matrix (Sudek and Kay, 2003). AGEs are the result of a non-enzymatic reaction between amino acids (mainly lysine and arginine) and reducing sugars

(e.g. threose) (Chen et al., 2002). The fact that the enhancement of AGEs accumulation makes the cartilage matrix stiffer and prone to fatigue failure is well described and is thought to be the result of increased collagen cross-linking (Verzijl et al., 2002). Since the biomechanical function of articular cartilage is under the control of chondrocytes, AGEs-related modifications may vary the chondrocytes' metabolism and alter the normal tissue turnover which eventually predisposes the cartilage tissue to OA (DeGroot et al., 2001).

Understanding the effects of AGEs on the cartilage matrix requires insight into how the biomechanical responses of various cartilage components are affected by AGEs. There is, however, not much data available in the literature as to how glycation influences the micro- and nano-mechanics of the cartilage (constituents). The overall aim of this study is to improve understanding of the effect of non-enzymatic glycation at both micro- and molecular levels in order to track the effect of AGEs on each cartilage component. In this study, we simulated the aging effect in rat knee cartilage using L-threose (in vitro). L-threose is a

* Correspondence to: Department of Orthopaedics, UMC Utrecht, Uppsalalaan 8, PO Box 85500, 3508 GA, 3584 CT Utrecht, The Netherlands.

E-mail addresses: p.rahnamamoshtagh@umcutrecht.nl (P.R. Moshtagh), n.m.korthagen@uu.nl (N.M. Korthagen), M.Rijen@umcutrecht.nl (M.H.P. van Rijen), r.m.castelein@umcutrecht.nl (R.M. Castelein), a.a.zadpoor@tudelft.nl (A.A. Zadpoor), h.h.weinans@umcutrecht.nl (H. Weinans).

<http://dx.doi.org/10.1016/j.jmbbm.2017.09.035>

Received 27 April 2017; Received in revised form 16 September 2017; Accepted 27 September 2017

Available online 30 September 2017

1751-6161/ © 2017 Elsevier Ltd. All rights reserved.

highly reactive carbohydrate that interacts with the cartilage matrix and increases the cross-linking of collagen, resulting in marked brownish color change (Saudek and Kay, 2003). We detected the resulting mechanical changes in both cartilage tissue (i.e. micro-scale) and the molecular constituents (i.e. nano-scale) respectively using micro-indentation and indentation-type atomic force microscopy.

2. Materials and methods

2.1. Sample harvesting and cross-linking

Intact knee joints were obtained from six 12-week-old male rats (Harlan Laboratories, Horst, Germany). Cartilage samples with underlying bone (~ 5 mm) were taken from the left (as control) and right (as test/crosslinking induced) femoral condyles of the same rat joint and stored at -20°C . In order to induce cross-linking, the test cartilage was incubated with a solution of 100 mM L-threose (Sigma-Aldrich, Zwijndrecht, the Netherlands) in phosphate buffer solution (PBS, Gibco, UK) for 7 days at 37°C , while the control cartilage was incubated in PBS only. Both solutions contained protease inhibitors (complete, Roche, Mannheim, Germany).

2.2. Biomechanical testing

2.2.1. Micro-scale indentation

Micro-indentations were performed on both test and control samples before (at day 0) and after the incubation (at day 7) using a microindenter machine (Piima, The Netherlands) with a controller (Optics, The Netherlands) and a spherical indenter (radius: $48\ \mu\text{m}$, cantilever stiffness: $65.7\ \text{N/m}$). The Piima indenter is referred to as a nanoindenter, but in fact this is not a correct representation as it yields micro-scale mechanical properties of the material. The applied indentation protocol was composed of a loading phase for 1 s at $18\ \mu\text{m}$ indentation depth, which was held for 7 additional seconds, and then an unloading phase for 20 s. The actual indentation displacement is always lower than selected in the indentation profile, because the indentation depth that is selected is a combination of the cantilever deflection and the desired depth of indentation across the cartilage thickness (Moshtagh et al., 2016a). Before starting the experiments, signal calibration was performed and the geometrical factors of the probes were calibrated. Indentation measurements were done at a 9×9 grid within a region around $500 \times 500\ \mu\text{m}^2$ ($65\ \mu\text{m}$ distance between each point, $n = 81$) at the central portion of the rat lateral femoral condyle ($n = 5$). The effective elastic modulus was calculated based on the Oliver-Pharr theory using the unloading force-displacement curves (Eq. (1)) (Oliver, 1992).

$$E_r = \frac{\frac{dp}{dh}}{2r^{1/2}\sqrt{h_{\max} - h_{\text{final}}}} \quad (1)$$

where P is the load, h is the displacement (indentation) and $\frac{dp}{dh}$ represents the slope of the initial part of the unloading curve in the load-displacement curve, r is the indenter radius, h_{\max} and h_{final} are respectively maximum indentation and final unloading depths, and E_r is the effective elastic modulus. See Moshtagh et al. (2016a) for a more detailed description of this test.

In order to compare the mechanical properties measured at micro-scale, a one-way ANOVA followed by post-hoc analysis was performed using MATLAB with $p < 0.05$ as the statistical significance threshold.

2.2.2. Nano-scale indentation

Indentation-type atomic force microscopy (IT-AFM) was performed using a nanoscope controller (Bruker, Dimension V, Japan) with a standard fluid cell (Bruker) to obtain the indentation-based force-displacement curves. A nano-scale pyramidal tip (radius: $15\ \text{nm}$, cantilever spring constant: $0.06\ \text{N/m}$) (Nano and More, Germany) was utilized.

The actual value of the cantilever spring constant was determined using the thermal tune method (Notbohm et al., 2011). Indentations were performed at day 0 and day 7 on the left (control) and right (treated) femoral condyle of only one animal, due to time constraints. Around 800 measurements were done at a $3\ \text{Hz}$ frequency corresponding with an indentation rate of $3\ \mu\text{m/s}$ and a depth of $500\ \text{nm}$ (Moshtagh et al., 2016b). A Poisson ratio of 0.5 was adopted in accordance with the incompressibility assumption (Jin and Lewis, 2004). The Young's modulus was calculated using the Nanoscope analysis software (Bruker, version 1.4) based on the Sneddon's indentation theory (Eq. (2)) (Oliver, 1992). The histogram of the measured stiffness values (converted to probability density function) was analyzed using the four-component finite Gaussian mixture model (Zadpoor, 2015), which fits a weighted sum of multiple Gaussian distributions to the obtained raw data (Eq. (3)).

$$P = \frac{\pi \tan \varphi}{2\gamma^2} \frac{E}{1 - \nu^2} h^2 \quad (2)$$

In the above equation, φ is the half angle of the cone, ν is the Poisson's ratio, and $\gamma = \pi/2$.

$$f(x) = \sum_{i=1}^m w_i N(\mu_i, \sigma_i) \quad (3)$$

where $f(x)$ is the probability distribution function and $N(\mu_i, \sigma_i)$ is the Gaussian probability. The mean, standard deviation, and weighting factor of each constituent (i) are respectively denoted by μ_i , σ_i , and w_i .

2.3. Histological examination

Knee joints were fixed in formaldehyde (4%, Klinipath, The Netherlands) for 2 days. Afterwards, the samples were decalcified with EDTA solution (12.5%, VWR, Belgium) for 21 days. They were then processed by means of graded ethanol steps to xylene, infiltrated and embedded in paraffin. Tissue sections with $5\ \mu\text{m}$ thickness were sliced perpendicular to the cartilage surface using a microtome (Thermo scientific Micron HM 340E, Germany). Safranin-O staining with a fast green was used to stain the microscopic slides of the knee joints. They were then visualized using a light microscope (Olympus BX51, Japan).

3. Results

There were clear differences in the surface colors between the samples and the L-threose treated specimens became yellow-brown after 7 days of sugar incubation (Fig. 1a). More than 3-fold changes in the cartilage micro-stiffness before and after L-threose incubation were detected by micro-indentation (Table 1, control at day 7 vs. test at day 7). Comparing micro-scale data before and after incubation, shows relatively 2-fold decrease in the effective elastic modulus for the control (left) knees and 2-fold increase for L-threose treated right knees (test, Table 1). Although we observed variations over each sample (Fig. 1b), the difference between the average modulus of controls between day 0 and 7 was $-55.4 \pm 14.1\%$, while the difference between test samples before (day 0) and after sugar incubation (day 7) was $+92.8 \pm 95.1\%$. The micro-scale modulus of the L-threose-treated group (at day 7) was significantly different from their initial value (at day 0) as well as from the controls (only with PBS treated) at day 7 ($p = 0.002$). The actual indentation depths for control and test samples were respectively between $3.5\text{--}9\ \mu\text{m}$ and $1.5\text{--}6\ \mu\text{m}$. Despite a large spatial variability of the modulus across the cartilage surface layer, quite similar (average) micro-stiffness with less than 18% changes between left and right knee joints for each rat at day 0 was observed (Fig. 1b). This indicates that applying a large number of indentations tests in accordance with the previously defined guidelines (Moshtagh et al., 2016a), indeed reduces the impact of intrinsic topographic variation.

For the nanoindentation using AFM, the Gaussian mixture model

Download English Version:

<https://daneshyari.com/en/article/7207384>

Download Persian Version:

<https://daneshyari.com/article/7207384>

[Daneshyari.com](https://daneshyari.com)